J|A|C|S
ARTICLES
Published on Web 05/26/2006

Phosphate Activation in the Ground State of Purine Nucleoside Phosphorylase

Hua Deng,* Andrew S. Murkin, and Vern L. Schramm

Contribution from the Department of Biochemistry, Albert Einstein College of Medicine, 1300 Morris Park Avenue, Bronx, New York 10461

Received October 15, 2005; E-mail: hdeng@aecom.yu.edu

Abstract: Phosphate and ribose 1-phosphate (R1P) bound to human purine nucleoside phosphorylase (PNP) have been studied by FTIR spectroscopy for comparison with phosphate bound with a transition state analogue. Bound phosphate is dianionic but exists in two distinct binding modes with similar binding affinities. The phosphate of bound R1P is also dianionic. Bound R1P slowly hydrolyzes to ribose and phosphate even in the absence of nucleobase. The C−OP bond is cleaved in bound R1P, the same as in the PNP-catalyzed reaction. Free R1P undergoes both C−OP and CO−P solvolysis. A hydrogen bond to one P···O group is stronger than those to the other two P···O groups in both the PNP·R1P complex and in one form of the PNP·PO_4 complex. The average hydrogen bond strength to the P···O bonds in the PNP·R1P complex is less than that in water but stronger than that in the PNP·PO_4 complex. Hydrolysis of bound R1P may be initiated by distortion of the phosphate moiety in bound R1P. The unfavorable interactions on the phosphate moiety of bound R1P are relieved by dissociation of R1P from PNP or by hydrolysis to ribose and phosphate. The two forms of bound phosphate in the PNP·PO_4 complex are interpreted to be phosphate positioned as the product in the nucleoside synthesis direction and as the reactant in the phosphorolysis reaction; their interconversion can occur by the transfer of a proton from one PO bond to another. The electronic structure of phosphate bound with a transition state analogue differs substantially from that in the Michaelis complexes.

Introduction

Phosphoryl transfer enzymes function by either breaking the bridging RO−P bond so that a PO_3 group is transferred or breaking the R−OP bond so that a PO_4 group is transferred. The phosphate distortions in the reaction intermediate by several PO_3 transferring enzymes have been studied. For example, the structure of a cryo-temperature trapped, pentacovalent phosphorus intermediate in β-phosphoglucomutase has been observed by X-ray crystallography.[1,2] By using photolysis of caged GTP bonds, the distortions of the phosphate moiety during the hydrolysis of GTP in Ras protein activated by GTPase activating protein or in a hyper-active mutant have been studied by FTIR.[3,4] Similar studies have been performed on the phosphate distortion in ATP hydrolysis by Ca^{2+}−ATPase using caged ATP compounds.[5] These studies revealed how the phosphate moieties in Ras and Ca^{2+}−ATPase are distorted to facilitate the hydrolysis reaction.

In this study, we report the observation of phosphate distortion in ground state complexes of another class of phosphoryl transferring enzyme, purine nucleoside phosphorylase (PNP).[6] It has been suggested that this reaction proceeds by a mechanism termed "nucleophilic displacement by electrophile migration" (see below). Previous X-ray crystallography studies on a transition state analogue complex have shown that in this mechanism the nucleophilic inorganic phosphate is fixed in the catalytic site pocket by at least nine hydrogen bonds and ionic interactions with the protein and an additional hydrogen bond and ionic interaction with Immucillin-H, a transition state analogue.[7,8] These interactions decouple the stretch motion of one P···O stretch of the bound phosphate from the other two, resulting in a highly asymmetric bound phosphate.[9] Here we investigate the nature of bound phosphate in the Michaelis complexes of phosphate and ribose 1-phosphate without the transition state analogue. Comparison of these complexes suggests changes to the phosphate environment on conversion from Michaelis to transition state analogue complexes.

Purine nucleoside phosphorylase catalyzes the reversible phosphorolysis of the N-ribosidic bond of 6-oxypurine nucleosides and deoxynucleosides (Scheme 1). In humans, the metabolic role of PNP is to remove deoxyguanosine that accumulates from DNA turnover. The genetic deficiency of PNP

(1) Tremblay, L. W.; Zhang, G.; Dai, J.; Dunaway-Mariano, D.; Allen, K. N. *J. Am. Chem. Soc.* **2005**, *127*, 5298−9.
(2) Lahiri, S. D.; Zhang, G.; Dunaway-Mariano, D.; Allen, K. N. *Science* **2003**, *299*, 2067−71.
(3) Allin, C.; Gerwert, K. *Biochemistry* **2001**, *40*, 3037−46.
(4) Du, X.; Frei, H.; Kim, S. H. *J. Biol. Chem.* **2000**, *275*, 8492−500.
(5) Liu, M.; Krasteva, M.; Barth, A. *Biophys. J.* **2005**, *89*, 4352−63.
(6) Abbreviations: PNP, human purine nucleoside phosphorylase; R1P, α-D-ribose 1-phosphate; ImmH, Immucillin-H.
(7) Fedorov, A.; Shi, W.; Kicska, G.; Fedorov, E.; Tyler, P. C.; Furneaux, R. H.; Hanson, J. C.; Gainsford, G. J.; Larese, J. Z.; Schramm, V. L.; Almo, S. C. *Biochemistry* **2001**, *40*, 853−60.
(8) Lewandowicz, A.; Shi, W.; Evans, G. B.; Tyler, P. C.; Furneaux, R. H.; Basso, L. A.; Santos, D. S.; Almo, S. C.; Schramm, V. L. *Biochemistry* **2003**, *42*, 6057−66.
(9) Deng, H.; Lewandowicz, A.; Schramm, V. L.; Callender, R. *J. Am. Chem. Soc.* **2004**, *126*, 9516−7.

10.1021/ja0570281 CCC: $33.50

Scheme 1. PNP-Catalyzed Reaction and ImmH−Phosphate Interactions in the PNP·ImmH·PO_4 Complex

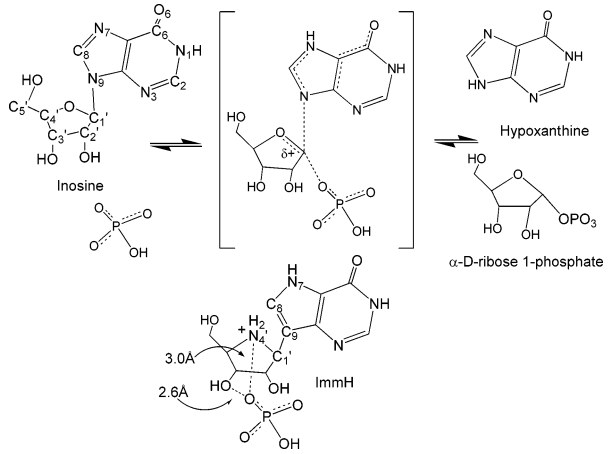

causes a T-cell immunodeficiency due to dGTP accumulation in dividing T-cells.[10] Inhibition of PNP inhibits the growth of activated T-cells, providing a clinical means to ameliorate T-cell proliferative disorders.[11] The catalytic acceleration of PNP is achieved through formation of a transition state with oxacarbenium ion character and specific leaving group interactions to the purine. Ribosides with better leaving groups, such as 4-nitrophenyl-β-D-riboside, are poor substrates, establishing leaving group activation as a major catalytic interaction.[12] Catalytic site contacts to the purine fix it in one position through the reaction coordinate and facilitate ribosyl electrophile migration from the leaving group to a phosphorus nucleophile also immobilized at the catalytic site.[7] Although the reaction equilibrium favors nucleoside synthesis, the enzyme operates in the phosphorolysis direction in vivo because of the rapid metabolic removal of products by purine phosphoribosyl transferases.

Recently, nucleophilic displacement by electrophilic migration has been proposed for PNP, hypoxanthine-guanine (-xanthine) phosphoribosyl transferase, lysozyme, and uracil DNA glycosylase.[7,13] Key features of this S_N1 reaction mechanism include (1) activation of both leaving group and nucleophile, (2) activation of the nucleobase leaving group by protonation or by hydrogen bonding to N7, (3) formation of a fully dissociated ribooxacarbenium ion at some point (not necessarily the transition state) during the reaction, and (4) neighboring group assistance by stacking the ribose O5′ over O4′ as a driving force for the electrophile (ribooxacarbenium) migration in PNP. This reaction mechanism is significantly different from the S_N2-like mechanisms previously proposed for a wide range of glycosyl transferases, wherein activation of the nucleophile in the ground state is not required and no ribooxacarbenium ion is formed. Furthermore, the phosphate group is fixed in position relative to the enzyme, unlike that in the PO_3 transferring enzymes.

The formation of an enzyme-stabilized ribooxacarbenium ion requires significant substrate activation in the ground state, and hydrolytic quenching of oxacarbenium ions by water molecules in the active site might be expected. Previous studies have shown that bovine PNP catalyzes the hydrolysis of inosine in the absence of PO_4 and binds tightly to the hypoxanthine ($K_d \sim 2$ pM) product,[14] supporting the formation of a ribooxacarbenium ion and its subsequent hydrolysis. However, the observation of stable inosine in the crystal structures of a PNP·inosine complex seems to be inconsistent with the S_N1-like mechanism and in favor of a S_N2-like mechanism.[15] The recent transition state analysis of human PNP provides unequivocal evidence that the arsenolysis reaction catalyzed by PNP has a transition state closely related to a fully dissociated ribooxacarbenium ion.[16]

Vibrational spectroscopy is an ideal tool to probe the electronic state of enzyme-bound phosphate and its interactions with proteins.[4,17−21] Activation of phosphate in a transition state analogue complex of PNP·ImmH·PO_4 has been studied by vibrational spectroscopy and ab initio normal mode analysis.[9] To investigate how PNP may activate the phosphate nucleophile in the ground state, we have extended our vibrational studies to the PNP·PO_4 and PNP·R1P complexes. Our results show that the phosphate dianions in both complexes are noticeably distorted upon binding to PNP, established by significant frequency changes in the phosphate P···O stretch modes. Furthermore, we have found that bound R1P is slowly hydrolyzed to ribose and phosphate by attack of the water (hydroxyl) nucleophile at C1 of R1P, rather than at the phosphorus atom. This reaction resembles the PNP-catalyzed nucleoside synthesis reaction. Thus, activation of the substrate R1P toward the ribooxacarbenium ion in the PNP·R1P complex is evidence for the ground state activation expected in the electrophile migration mechanism. Substrate activation arises from the unfavorable interactions on the phosphate moiety of PNP-bound R1P compared to either PNP-bound phosphate or R1P in solution.

Materials and Methods

7-Methyl inosine was obtained from Sigma. $H_3P^{18}O_4$ was prepared according to the published procedure.[22] R1P or $^{18}O_4$-labeled R1P was prepared by mixing PO_4 or $P^{18}O_4$ and 7-methyl inosine in a 1:1.5 molar ratio at pH 7.5 in the presence of PNP. After completion of the reaction, the unreacted nucleoside and base were removed by charcoal. The final products were checked by ^{1}H and ^{31}P NMR to be >99% pure and free of inorganic phosphate. Human PNP was prepared as described previously.[23] To remove tightly bound hypoxanthine that co-purifies with human PNP, the enzyme (at concentration <1 mg/mL, determined by UV using an extinction coefficient of 30 mM^{-1} cm^{-1} at 280 nm) was dialyzed for 3 days against 50 mM phosphate buffer at pH 7.2, 4 °C in the presence of 2 g of charcoal in the dialysate. Removal of bound hypoxanthine was verified with proton NMR.[24] Hypoxanthine-

(10) Stoeckler, J. D. Developments in Cancer Chemotherapy. In *Developments in Cancer Chemotherapy*; Glazer, R. J., Ed.; CRC Press Inc.: Boca Raton, FL, 1984; pp 35−60.
(11) Bzowska, A.; Kulikowska, E.; Shugar, D. *Pharma. Ther.* **2000**, *88*, 349−425.
(12) Mazzella, L. J.; Parkin, D. W.; Tyler, P. C.; Furneaux, R. H.; Schramm, V. L. *J. Am. Chem. Soc.* **1996**, *118*, 2111−2.
(13) Schramm, V. L.; Grubmeyer, C. *Prog. Nucleic Acid Res. Mol. Biol.* **2004**, *78*, 261−304.
(14) Kline, P. C.; Schramm, V. L. *Biochemistry* **1992**, *31*, 5964−73.
(15) Canduri, F.; dos Santos, D. M.; Silva, R. G.; Mendes, M. A.; Basso, L. A.; Palma, M. S.; de Azevedo, W. F.; Santos, D. S. *Biochem. Biophys. Res. Commun.* **2004**, *313*, 907−14.
(16) Lewandowicz, A.; Schramm, V. L. *Biochemistry* **2004**, *43*, 1458−68.
(17) Mertz, E. L.; Leikin, S. *Biochemistry* **2004**, *43*, 14901−12.
(18) Martinez-Liarte, J. H.; Iriarte, A.; Martinez-Carrion, M. *Biochemistry* **1992**, *31*, 2712−19.
(19) Wang, J. H.; Xiao, D. G.; Deng, H.; Webb, M. R.; Callender, R. *Biochemistry* **1998**, *37*, 11106−16.
(20) Cheng, H.; Sukal, S.; Deng, H.; Leyh, T. S.; Callender, R. *Biochemistry* **2001**, *40*, 4035−43.
(21) Chakrabarti, P. P.; Suveyzdis, Y.; Wittinghofer, A.; Gerwert, K. *J. Biol. Chem.* **2004**, *279*, 46226−33.
(22) Deng, H.; Wang, J.; Ray, W. J.; Callender, R. *J. Phys. Chem. B* **1998**, *102*, 3617−23.
(23) Deng, H.; Lewandowicz, A.; Cahill, S. M.; Furneaux, R. H.; Tyler, P. C.; Girvin, M. E.; Callender, R. H.; Schramm, V. L. *Biochemistry* **2004**, *43*, 1980−7.
(24) Deng, H.; Cahill, S. M.; Abad, J. L.; Lewandowicz, A.; Callender, R. H.; Schramm, V. L.; Jones, R. A. *Biochemistry* **2004**, *43*, 15966−74.

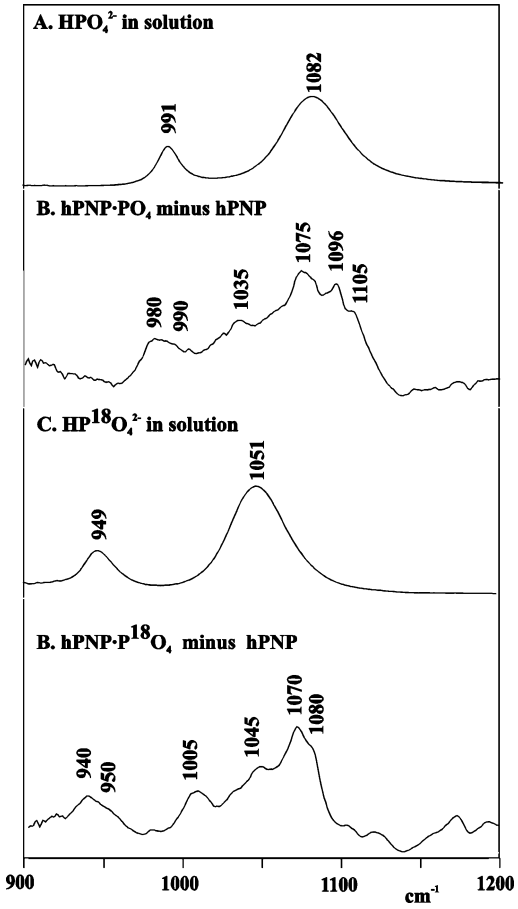

Figure 1. (A) FTIR spectrum of 50 mM HPO_4^{2-} at pH 9.5. (B) FTIR difference spectrum of PNP·PO_4 complex minus PNP at pH 7.5 at room temperature. (C) FTIR spectrum of 50 mM $[^{18}O_4]HPO_4^{2-}$ at pH 9.5. (D) FTIR difference spectrum of PNP·$[^{18}O_4]PO_4$ complex minus PNP at pH 7.5 at room temperature. Only nonbridging P···O stretch modes are observed in the 900−1200 cm^{-1} spectral range. The enzyme samples were prepared in 300 mM NaCl. The concentration of PNP:PO_4 in these complexes was 4:3.5 mM.

free PNP was dialyzed against 0.3 M NaCl at pH 7.0 to remove phosphate and concentrated to ∼4 mM by Centricon30 for IR measurements.

FTIR spectroscopy was performed on a Magna 760 Fourier transform spectrometer (Nicolet Instrument Corp., WI) using a MCT detector. BaF_2 windows with a 25 μm Teflon spacer were used. Spectra were collected in the range of 900−4000 cm^{-1} with 2 cm^{-1} resolution. A Blackman−Harris three-term apodization and a Happ−Genzel apodization were applied, respectively. Omnic 4.1a (Nicolet Instruments, Corp.) software was used for data collection and analysis.

Solution ^{31}P NMR spectra were obtained at 121.5 MHz on a Bruker DRX300 spectrometer; 2k scans were collected in each spectrum with a sweep width of 14 ppm, sampled with 8k points, and a recycle delay of 3.5 s.

Results

Phosphate Binding in the PNP·PO_4 Complex. For HPO_4^{2-} in water (at pH 9.5, >99% of PO_4 will be present as the dianion), the three P···O stretches are coupled to form a symmetric stretch at 991 cm^{-1} (Figure 1A) and a 2-fold degenerate asymmetric stretch mode at 1080 cm^{-1} (Figure 1A). Upon $^{18}O_4$ labeling of the phosphate, these vibrational frequencies show −34 and −32 cm^{-1} shifts for symmetric and asymmetric modes, respectively (Figure 1C). The difference spectrum between the PNP·PO_4 complex and PNP contains positive features due to P···O stretches of the bound phosphate and positive or negative features due to the protein vibrational modes that are shifted upon phosphate binding (Figure 1B). Since Figure 1B and 1D clearly shows more than three phosphate modes, which is the maximum number of P···O stretch bands that can be observed for a phosphate in this spectral region, we conclude that there are more than one binding mode for the PNP-bound phosphate. The simplest interpretation of the spectra of PNP-bound phosphate is that there are two binding modes, resulting in a maximum of six P···O stretches. P···O stretch bands can be identified by their frequency shifts upon ^{18}O labeling of the phosphate with the constraint that the isotope shift should be in the range of 25−45 cm^{-1}. On the basis of these criteria, six bands at 980, 990, 1035, 1075, 1096, and 1105 cm^{-1} in Figure 1B can be assigned to the phosphate P···O stretches on the basis of their ^{18}O shifts (Figure 1D). Since the intensities of the two symmetric P···O stretches at 980 and 990 cm^{-1} are similar, indicating similar populations, the binding affinities of the two types of phosphate should also be similar. Further attempts to assign these P···O stretches to one or the other form of bound phosphate by exploring different PO_4 binding affinities did not yield conclusive results because of insufficient signal-to-noise at low phosphate concentrations. Nevertheless, the observation of a P···O stretch band at 1035 cm^{-1}, which is 45 cm^{-1} lower than the asymmetric P···O stretch in solution, is consistent with one form of bound phosphate having a P···O bond more strongly hydrogen bonded than the other two P···O bonds (see below). In the other form of bound phosphate, all three P···O bonds experience similar hydrogen bonding strength, resulting in two near degenerate asymmetric P···O stretches with similar frequencies.

Phosphate Binding in the PNP·R1P Complex. Our first attempt to obtain the isotope-edited difference FTIR spectrum of PNP·R1P failed, yielding a difference spectrum that was similar to the bound phosphate spectrum shown in Figure 1B. PNP slowly decomposes R1P to ribose and phosphate, as confirmed by ^1H and ^{31}P NMR measurements (data not shown). This reaction is not due to trace contaminants of phosphomonoesterase since the reaction is stopped by the addition of the specific PNP inhibitor Immucillin-H. Fortunately, R1P hydrolysis is slow enough to permit FTIR experiments to be completed with appropriate precautions.

Figures 2A and 3A show the FTIR spectra of R1P and ^{18}O-labeled R1P, respectively, in solution. At pH 9.0, R1P was stable for the time of the measurement, and at this pH, >99% of the phosphate group is dianionic. The R1P bands at 950 and 1095 cm^{-1} (Figure 2A) can be assigned to the symmetric and the asymmetric P···O stretch modes, respectively, based on the ^{18}O shifts (28 cm^{-1} for both modes; Figure 3A). It is interesting to note that these frequencies are significantly different from those of the dianionic phosphate P···O stretches in solution (Figure 1A). Figure 2B shows the time evolution of the PNP·R1P spectra from 1 to 20 min after mixing. These spectra were obtained by collecting sequential FTIR spectra and by dividing each spectrum by the last one. Division (rather than subtraction) provides more consistent baselines to identify both positive and negative bands, whose intensities decrease with time using this difference procedure. The positive features are related to the PNP·R1P complex, and the negative features are related to the PNP·PO_4 complex. Thus, the phosphate P···O stretch bands of

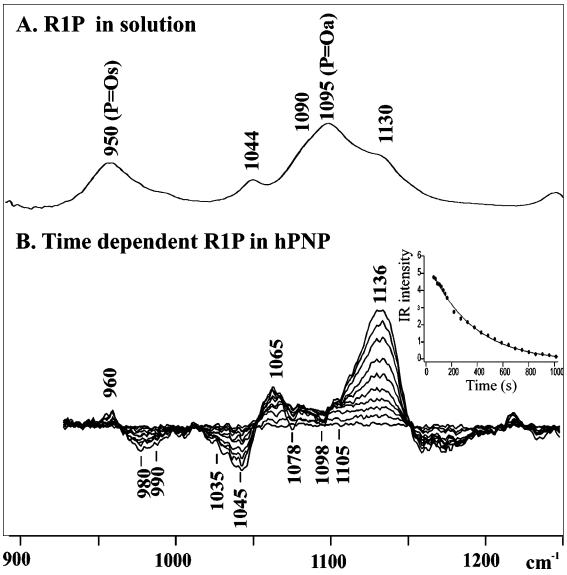

Figure 2. (A) FTIR spectrum of 50 mM R1P at pH 9.0. R1P is stable at this pH for days. (B) The time-dependent, serial difference FTIR spectra of the PNP·R1P complex at pH 7.0. The first spectrum was recorded about 1 min after mixing, the following seven spectra were recorded at 14 s intervals, and the subsequent 18 spectra were recorded at 55 s intervals. Difference spectra were constructed by dividing each of the spectra by the last one. Selected spectra are presented here. In this form, difference spectra present the vibrational modes of bound R1P as positive bands, while the vibrational modes of the ribose and phosphate products appear as negative bands. All band intensities decrease with time and disappear as the reaction reaches equilibrium. The inset to B shows a single-exponential curve fitted to the time dependence of the band intensity at 1136 cm^{-1}. The average time constant determined from several measurements, including those with [$^{18}O_4$]R1P, is 0.023 ± 0.005 s^{-1}. The concentration of PNP:R1P in the complex was 4:4 mM.

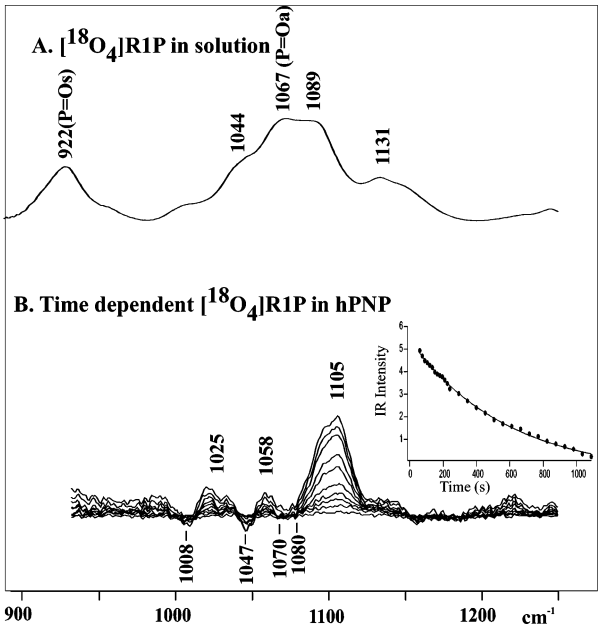

Figure 3. (A) FTIR spectrum of 50 mM [$^{18}O_4$]R1P at pH 9.0. (B) Same as in Figure 2B except [$^{18}O_4$]R1P is used.

bound R1P are positive, while the P···O stretch bands of bound PO_4 are negative. Protein bands can appear either as positive or negative because some protein vibrational modes change when R1P is hydrolyzed to ribose and phosphate.

The major positive band at 1136 cm^{-1} is assigned to the asymmetric P···O stretch of bound R1P based on its 31 cm^{-1} ^{18}O shift (to 1105 cm^{-1} in Figure 3B). A component of the 1065 cm^{-1} band is assigned to another asymmetric P···O stretch based on its decreased intensity and the appearance of a new broad band near 1025 cm^{-1} upon ^{18}O labeling of R1P (Figure 3B). The 960 cm^{-1} band in the spectra of PNP·R1P is assigned to the symmetric P···O stretch. Due to strong absorbance of the IR window material and water below 950 cm^{-1}, this stretch band could not be observed for the PNP·R1P complex with ^{18}O-labeled R1P. However, disappearance of this band upon ^{18}O labeling of R1P is consistent with the assignment (Figure 3B). Many of the negative bands in Figure 2B are associated with the P···O stretch modes of bound phosphate. Their counterparts are readily identified in the bound phosphate spectrum (PNP·PO_4; Figure 1B). Thus, both kinds of difference spectra (Figures 1B and 2B) are consistent with two phosphate binding modes in the PNP·PO_4 complex. The symmetric P···O stretch of R1P shifts up by 10 cm^{-1} upon binding to PNP, and the two asymmetric P···O stretches shift in opposing directions by −30 and +41 cm^{-1} in the PNP·R1P complex (Figure 2A and 2B).

The time evolutions for the major asymmetric P···O stretch band at 1136 cm^{-1} of unlabeled R1P and the 1105 cm^{-1} band of the ^{18}O-labeled R1P fit to a single-exponential function (insets of Figures 2B and 3B), yielding a rate constant of 0.023 ± 0.005 s^{-1} for PNP-catalyzed hydrolysis of R1P.

The Nature of the PNP-Catalyzed Decomposition of R1P. Two mechanisms could account for R1P conversion to ribose and phosphate: the bond cleavage of the CO−P bond or the C−OP bond. It is important to determine the reaction mechanism since, in the latter case, the distortion of the phosphate moiety of R1P in the PNP·R1P complex should be similar to that in the PNP·base·R1P complex in the direction of nucleoside synthesis.

These two cases can be distinguished by ^{31}P NMR measurements of the phosphate product from the PNP-catalyzed R1P decomposition using ^{18}O-labeled R1P.[25] Each ^{18}O labeling of the four phosphate oxygens causes a ∼0.02 ppm upfield shift of the ^{31}P chemical shift.[26] The ^{31}P spectrum for a mixture of unlabeled and ^{18}O-labeled phosphate (3:1 molar ratio) shows a small resonance ∼0.02 ppm downfield of the major ^{18}O-labeled phosphate resonance, consistent with <10% of the ^{18}O-labeled phosphate with three ^{18}O atoms (Figure 4A). The number of the ^{18}O atoms on the phosphate product from R1P with PNP was determined by a ^{31}P measurement of the mixture of this product (Figure 4B) and the known phosphate sample (Figure 4A). The major resonance of the products of ^{18}O-labeled R1P from PNP overlaps with the $P^{18}O_4$ resonance in the mixture, establishing that it contains phosphate with four ^{18}O atoms (Figure 4C). Thus, the PNP-catalyzed decomposition of R1P occurs by the cleavage of the C−OP bond, as in the PNP-catalyzed nucleoside synthesis reaction. The nonenzymatic hydrolysis of R1P in aqueous solution, pH 9.0, at 80 °C, involves cleavage at both C−OP and CO−P bonds, resulting in equal amounts of $P^{18}O_4$ and $PO^{18}O_3$ (Figure 4D and 4E).

Discussion

Phosphate Structure from Vibrational Spectroscopy. Vibrational spectroscopy is a powerful tool to determine the

(25) Jordan, F.; Patrick, J. A.; Salamone, S., Jr. *J. Biol. Chem.* **1979**, *254*, 2384−6.
(26) Cohn, M.; Hu, A. *Proc. Natl. Acad. Sci. U.S.A.* **1978**, *75*, 200−3.

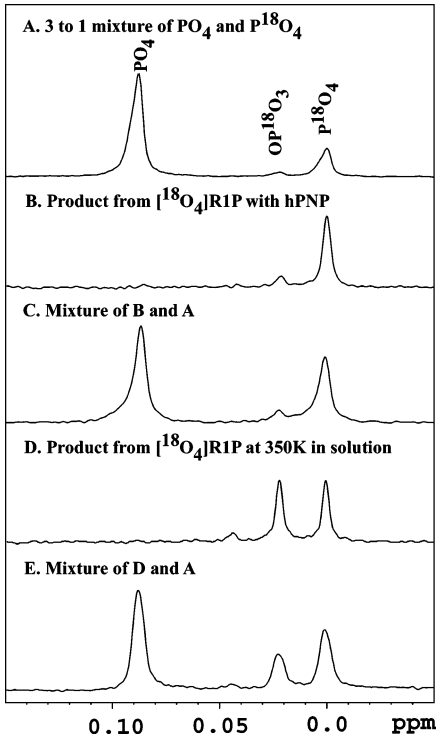

Figure 4. (A) 30:10 mM mixture of phosphate and ^{18}O-labeled phosphate. Sample contains 0.3 M NaCl and 2 mM EDTA. (B) The decomposition product of R1P by PNP. EDTA was added to a final concentration of 2 mM. The sample concentration was 10 mM. (C) ^{31}P spectrum of the sample mixture of A and B. (D) The hydrolysis product of 10 mM R1P at 80 °C at pH 9.0 for 18 h. EDTA was added to a final concentration of 2 mM prior to NMR measurements. (E) ^{31}P spectrum of the sample mixture of A and D.

ionization state of phosphate under various environments, especially in proteins, since the vibrational frequencies of the P···O stretches are significantly different in each ionic state (for recent applications, see refs 17 and 18). For P···O bonds of phosphates, vibrational normal mode analysis has provided very accurate empirical relationships for bond lengths ($R_{P\cdots O}$) and bond orders ($S_{P\cdots O}$) as a function of vibrational frequency.[22] They are given by $R_{P\cdots O} = [0.2838 \times \ln(224500/\upsilon)]$ and $S_{P\cdots O} = [0.175 \times \ln(224500/\upsilon)]^{-4.29}$, where υ is the average frequency of the phosphate stretches defined as $\upsilon^2 = (\upsilon_s^2 + n_a\upsilon_a^2)/(n_a + 1)$, where υ_s, υ_a, and n_a are the symmetric modes, asymmetric modes, and the degeneracy of υ_a, respectively. For dianionic phosphate, $n_a = 2$. The error in the bond length/frequency relationships in determining $R_{P\cdots O}$ is estimated to be about $\pm$0.004 Å, and bond orders (in valence units) to $\pm$0.04 vu.[19,22] In addition, bond angle changes, as a measure of the flatness of the $-PO_3^{2-}$ moiety, can also be estimated from the P···O stretch frequency changes.[19,22]

Phosphate Structure in a Transition State Analogue Complex. In a previous study, the bond lengths of the P···O bonds for HPO_4^{2-} in solution and in complex with a transition state analogue, ImmH, were characterized.[9] One of the P···O bonds in the PNP·ImmH·PO_4 complex is strongly polarized and is ~0.027 Å longer than the other two P···O bonds. The bond polarization is attributed to a ~3.0 Å ion pair interaction with N4′ of ImmH,[8,27] which is a cation.[28] Additional hydrogen bonds between PO_4 and active site residues also contribute.[9] In the following sections, similar analyses are performed on the data obtained with the PNP·PO_4 and PNP·R1P complexes.

Comparison of the Structures of the $-PO_3^{2-}$ Moiety in R1P and Phosphate. The P···O stretch frequencies in dianionic phosphate and in R1P are drastically different; the symmetric stretches differ by 41 cm^{-1} and asymmetric stretches differ by 15 cm^{-1} (Figures 1A and 2A). However, the average P···O stretch frequencies in these two compounds as defined above differ by only 2 cm^{-1}, corresponding to a very small change in the average bond order or bond length. The average P···O stretch frequency will be strongly influenced by the hydrogen bonding strength on the P···O bonds and, to a smaller extent, other factors such as the pK_a of the alcohol substituent.[29] Analysis using the methods given in Deng et al.[22] suggests that the $-PO_3^{2-}$ moiety is more flattened in R1P than in dianionic phosphate, and this geometry is largely responsible for the P···O stretch frequency pattern difference in these molecules. The geometry change does not cause a large change in the average P···O stretch frequency but does cause a significant change in the difference between symmetric and asymmetric P···O stretch frequencies. When the $-PO_3^{2-}$ moiety becomes more flattened, the frequency difference becomes larger. Molecular modeling calculations based on ab initio methods suggest that a hydrogen bond between the ribose C2−OH and one of the P···O bonds in R1P is likely to cause this geometry change.

PO_4 Distortion in the PNP·PO_4 Complex. Phosphate is distorted in the ternary complex of PNP with ImmH,[9] and the current study investigates distortion of phosphate and R1P in the binary complexes. From the six observed P···O stretch frequencies, we detect two dianionic forms of PO_4 bound to PNP. Although not all of the vibrational modes could be assigned, several important observations are noted as follows.

Normal mode calculations from phosphate model complexes indicate that a strong hydrogen bond to one of the P···O bonds causes the degenerate asymmetric P···O stretch band to split into two bands with frequencies higher and lower than the degenerate frequency. The stronger the hydrogen bonding, the larger the splitting becomes.[9] The P···O stretch mode at 1035 cm^{-1} in the complex is 45 cm^{-1} lower than the degenerate P···O stretch mode at 1080 cm^{-1} in solution. Thus, one of the P···O bonds in the first form of bound phosphate forms a stronger hydrogen bond than the rest of the P···O bonds. In the second form of the bound phosphate, the hydrogen bonds to all P···O bonds are similar so that the asymmetric P···O stretches are nearly degenerate. In the first form of bound phosphate, the average P···O stretch frequency is approximately 6 cm^{-1} lower than that in solution, establishing that the average hydrogen bonding to bound P···O bonds is stronger.[30] Since X-ray structures of PNP with bound phosphate reveal only one binding site for the PO_4 group (see below), the two forms of bound dianionic phosphate detected in our FTIR studies must locate

(27) Shi, W.; Basso, L. A.; Santos, D. S.; Tyler, P. C.; Furneaux, R. H.; Blanchard, J. S.; Almo, S. C.; Schramm, V. L. *Biochemistry* **2001**, *40*, 8204−15.

(28) Sauve, A. A.; Cahill, S. M.; Zech, S. G.; Basso, L. A.; Lewandowicz, A.; Santos, D. S.; Grubmeyer, C.; Evans, G. B.; Furneaux, R. H.; Tyler, P. C.; McDermott, A.; Girvin, M. E.; Schramm, V. L. *Biochemistry* **2003**, *42*, 5694−705.

(29) Cheng, H.; Nikolic-Hughes, I.; Wang, J. H.; Deng, H.; O'Brien, P. J.; Wu, L.; Zhang, Z. Y.; Herschlag, D.; Callender, R. *J. Am. Chem. Soc.* **2002**, *124*, 11295−306.

(30) This conclusion assumes that the higher symmetric stretch frequency and the highest asymmetric stretch are associated with this phosphate. If other frequencies are associated with this phosphate, the average frequency will be even lower, corresponding to even stronger hydrogen bonding.

Scheme 2. Hydrogen Bonding Distances to Phosphate in Selected Crystal Structures of PNP

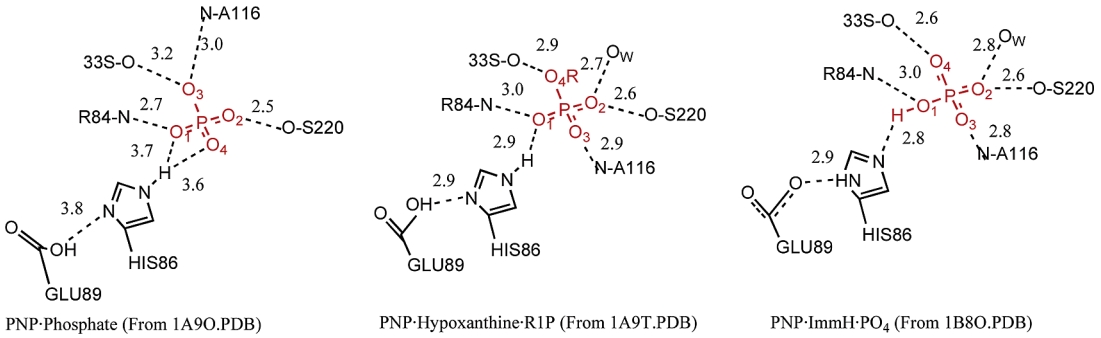

Scheme 3. Relative Hydrogen Bond Energy to $-PO_3^{2-}$ in Various Complexes Based on the Average P···O Stretch Frequency Changes from Solution

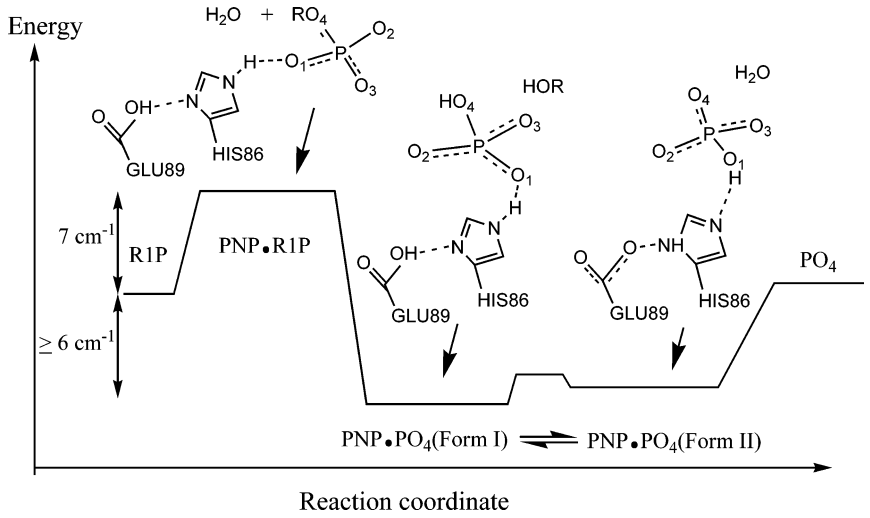

at the same place but differ only in their proton positions as discussed below.

Coordination with PNP Crystal Structures. The X-ray structures of PNP active sites reveal that several PNP active site residues and a structural water molecule interact with bound anions (Scheme 2; refs 7, 8, 31, and 32). One P···O bond is hydrogen bonded to the Nϵ2 of His86, while the carboxyl group of Glu89 is hydrogen bonded to the Nδ1 of His86 (Scheme 2). Similar triads, which involve an Asp/Glu-His pair and another titratable group, such as C−OH or P−OH, have been found in other enzymes and are proposed to form a proton relay channel. In PNP, this triad pattern allows the formation of a favorable hydrogen bond to the P···O1 and also allows a change of the protonation pattern for the bound phosphate dianion by proton relay to the Glu89 carboxyl group (Scheme 2). The protonation sites of phosphate are important since, in the phosphorolysis direction, the phosphate nucleophile requires the O4 to be an anion adjacent to the incoming oxacarbenium ion, while in the nucleoside synthesis direction, the PO_4 leaving group of the PNP·R1P complex must accommodate extra electron density as the ribosyl group accepts the hypoxanthine nucleophile (see below).

PO_4 Distortion in the PNP·R1P Complex. The slow decomposition of R1P catalyzed by PNP provides a useful probe into the catalytic mechanism. The specific C−OP bond cleavage in this reaction strongly suggests that this reaction contains features that are characteristic of transition state stabilization leading to nucleophilic displacements at the cationic carbon of ribose in normal PNP catalysis. The FTIR spectra indicate that the phosphate moiety of bound R1P is dianionic. Of the three P···O stretch frequencies, the symmetric stretch is blue shifted by 10 cm^{-1}, one asymmetric stretch is blue shifted by 41 cm^{-1}, and the other is red shifted by 30 cm^{-1}, compared to their solution values. Normal mode analysis based on ab initio frequency calculations of phosphate model compounds indicates that the breakdown of the frequency degeneracy of the two asymmetric stretches can be explained by different hydrogen bond strengths to the three P···O bonds in the PNP·R1P complex.[9] The hydrogen bond to the P···O1 group from the Nϵ2 of His86 is proposed to be stronger than those to the other P···O bonds. The average P···O stretch frequency in the PNP·R1P complex is ∼7 cm^{-1} higher than that of R1P in solution. Considering that the average P···O bond order of R1P is higher when bound to the enzyme than in solution, the average hydrogen bonding strength to the P···O bonds is weaker in the enzyme than in water. On the basis of leaving group potential, this interaction would be expected to stabilize R1P from loss of phosphate when bound to the enzyme. It is illuminating to see that this does not occur since PNP catalyzes its hydrolysis.

Hydrogen Bond Patterns to PO_4 and R1P. The interaction pattern of the phosphate moiety in the PNP·R1P complex is similar to that of the first form of the bound phosphate in the PNP·PO_4 complex, meaning that the hydrogen bonding to one

(31) Erion, M. D.; Takabayashi, K.; Smith, H. B.; Kessi, J.; Wagner, S.; Honger, S.; Shames, S. L.; Ealick, S. E. *Biochemistry* **1997**, *36*, 11725−34.
(32) Mao, C.; Cook, W. J.; Zhou, M.; Koszalka, G. W.; Krenitsky, T. A.; Ealick, S. E. *Structure* **1997**, *5*, 1373−83.

of the P···O bonds is stronger than to the others. This similarity suggests that the $-PO_3^{2-}$ moiety in these complexes may experience the hydrogen bonds from the same active site residues. However, the average hydrogen bond strength to the P···O bonds in the PNP·R1P complex is weaker than to bound phosphate, as indicated by the >12 cm^{-1} higher average P···O stretch frequency compared to the first form of the bound phosphate. It is also weaker than that of the R1P in solution, as indicated by its 7 cm^{-1} higher average P···O stretch frequency. Unfavorable hydrogen bonding interactions to the $-PO_3^{2-}$ moiety indicate high potential energy relative to solution thus a thermodynamically unstabilized phosphate leaving group.

Implications for the Reaction Mechanism. Crystal structures of PNP suggest that the protonated Nϵ2 of His86 may form a variable-strength hydrogen bond with the P···O1 bond, while hydrogen bonds formed with other residues and a structural water molecule complete the catalytic site contacts for a stable, bound PO_4 moiety (Scheme 2).[7,16,33,34] The observed P···O frequency patterns in the complexes studied here suggest that, in the PNP·R1P complex, the PO_4 group is unfavorably bound, presumably due to the steric crowding imposed by the ribose moiety of R1P, thus unable to form hydrogen bonds with protein active site residues at full strength. After the decomposition of R1P, the PO_4 is fully hydrogen bonded and all hydrogen bond energy with the phosphate moiety is released. During this process, a proton from the active site water replaced the ribose group of R1P and the hydroxyl group of the water forms a bond with the leaving oxacarbenium ion. In our hypothesis, the first form of bound phosphate is the phosphate product in the purine nucleoside synthesis direction. By transferring a proton from the protonated Nϵ2 of His86 to its hydrogen bonded P···O1, and with the aid from water molecules in the active site, the bound phosphate is converted to the second form in which the P···O4 oxygen anion points toward the ribose C1, as suggested from the PNP·PO_4 complex (Scheme 3). The second form of bound phosphate serves as the nucleophile substrate in the phosphorolysis direction, and the P···O4 bond is available for the formation of the C1−OP bond. The incoming oxacarbenium ion polarizes the bond during the reaction, as established in the studies of the transition state complexes of PNP·ImmH·PO_4.[7,9] Thus, our vibrational studies of PNP ground state complexes and a transition state complex provide unique information on how the phosphate is activated along the reaction coordinate.

Acknowledgment. Supported by research grants GM068036, EB001958 (Robert Callender), and GM41916 (V.S.) from the NIH.

JA0570281

(33) de Azevedo, W. F., Jr.; Canduri, F.; dos Santos, D. M.; Silva, R. G.; de Oliveira, J. S.; de Carvalho, L. P.; Basso, L. A.; Mendes, M. A.; Palma, M. S.; Santos, D. S. *Biochim. Biophys. Res. Commun.* **2003**, *308*, 545−52.
(34) Mao, C.; Cook, W. J.; Zhou, M.; Federov, A. A.; Almo, S. C.; Ealick, S. E. *Biochemistry* **1998**, *37*, 7135−46.